Drift compression of an intense neutralized ion beam

P. K. Roy, S. S. Yu, E. Henestroza, A. Anders, F. M. Bieniosek, J. Coleman, S. Eylon, W. G. Greenway, M. Leitner, B. G. Logan and W. L. Waldron
Lawrence Berkeley National Laboratory, 1 Cyclotron Road, Berkeley, CA-94720, U.S.A

D. R. Welch and C. Thoma
ATK Mission Research, Albuquerque, New Mexico 87110-3946, U.S.A

A. B. Sefkow, E. P. Gilson, P. C. Efthimion and R. C. Davidson
Princeton Plasma Physics Laboratory, New Jersey 08543-0451, U.S.A.
(Dated: September 7, 2005)

Longitudinal compression of a velocity-tailored, intense neutralized K^+ beam at 300 keV, 25 mA has been demonstrated. The compression takes place in a 1-2 m drift section filled with plasma to provide space-charge neutralization. An induction cell produces a head-to-tail velocity ramp that longitudinally compresses the neutralized beam, enhancing the beam peak current by a factor of 50 and producing a pulse duration of about 3 ns. This measurement has been confirmed independently with two different diagnostic systems.

PACS numbers: 28.52, 29.17, 29.20, 29.27, 28.52, 41, 52, 94.20, 94.30

To create high energy density matter and fusion conditions, high power drivers, such as lasers, ion beams, and x-ray drivers, are needed to heat targets with pulses short compared to hydro-motion. Both high energy density physics and ion-driven inertial fusion require the simultaneous transverse and longitudinal compression of an ion beam to achieve high intensities.

Longitudinal compression of space-charge-dominated beams has been studied extensively in theory and simulations [1–6]. The compression is initiated by imposing a linear head-to-tail velocity tilt to a drifting beam. Longitudinal space-charge forces limit the beam compression ratio, the ratio of the initial to final current, to about ten in most applications. An experiment with five fold compression has been reported [7].

Recent theoretical models and simulations predict that much higher compression ratios ($\leq$100) can be achieved if beam compression takes place in a plasma-filled drift region in which the space-charge forces of the ion beam are neutralized [8, 9]. If the compressed pulse length t_p is dominated by the longitudinal beam temperature T_l, t_p is approximately given by

$$t_p = \frac{L}{v_l^2}\sqrt{\frac{2kT_l}{M}}, \qquad (1)$$

where v_l, L, M and k are the mean longitudinal beam velocity, drift length, mass of ion and Boltzmann constant, respectively. In this letter, temporal bunch compression of an intense ion beam is demonstrated using a neutralized drift section and a tilted velocity distribution.

Figure 1 shows a schematic of the Neutralized Drift Compression Experimental (NDCX) setup. The NDCX experiment uses the same front end as the earlier Neutralized Transport Experiments (NTX) [10–15]. It consists of a 300 keV, 25-milliamp K^+ beam from an alumino silicate source powered by a Marx generator. The beam produced from the source has a 6 μs flat-top. Four pulsed quadrupoles magnets used in NTX to control the beam envelope (beam radius and convergence angle) are retained for the present experiments on NDCX.

To provide the head-to-tail velocity tilt, an induction module with a variable voltage waveform is placed immediately downstream of the last quadrupole magnet. The induction cell consists of 14 independently-driven magnetic cores in a pressurized gas (SF_6) region that is separated from the vacuum by a conventional high voltage insulator. The waveforms applied to the 14 cores inductively add at the acceleration gap. Each core is driven by a thyratron-switched modulator. Because the modulator for each core can be designed to produce different waveforms and can be triggered independently, a variety of waveforms can be produced at the acceleration gap using the 14 discrete building blocks. The induction tilt voltage 'carves' out a $\sim$300 ns segment of the flat-top which compresses longitudinally as it drifts through a one-meter long plasma column.

The plasma column is formed by two pulsed aluminum cathodic arc sources [16] located at the downstream end. Each source is equipped with a 45^0 open-architecture macroparticle filter providing a flow of fully ionized aluminum plasma [17]. The two plasma flows are pointed at an angle of 45^0 towards the solenoidal column ($\sim$ 1kG, 7.6 cm diameter, and 1 m long). A significant fraction (>10%) of the plasma enters the solenoid, and drifts practically unattenuated through the entire column (the rest of the aluminum plasma condenses at the wall and thereby removed from the system). In most of the operating regimes, the plasma density ($\sim$ 5x10^{10} cm$^-$3) is at least a factor of 10 higher than the beam density. At the upstream end of the column, we have introduced a 'plasma stopper' consisting of two opposing dipoles of $\sim$1kG each, which inhibit the motion of plasma upstream into the induction gap and quadrupole focusing sections.

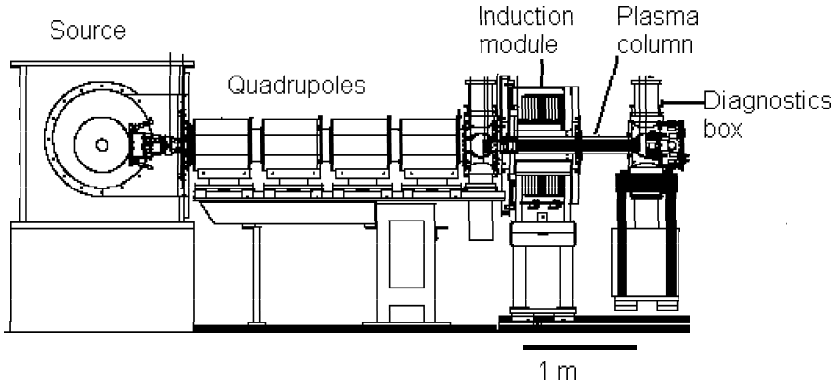

FIG. 1: Schematic of the NDCX experimental setup.

A second plasma column consisting of a meter-long ferroelectric plasma source that does not require solenoidal confinement has been constructed and is undergoing experimental tests. A diagnostic box is located at the downstream end of the plasma column. The final compressed beam is measured in the downstream diagnostic box.

A phototube diagnostic [18] is used to measure beam pulse compression with and without neutralization by background plasma. The optical system is based on a Hamamatsu phototube with fast (sub-ns) response which is coupled to a 500-MHz oscilloscope. The beam pulse is measured by using the phototube to collect the optical photon flux from an aluminum oxide scintillator placed in the path of the beam. The time response of the scintillator is fast enough to make measurements on a nanosecond time scale. Small amounts of stray light emitted by the plasma over long periods of time (100s of μs) can drain the bias charge in the phototube's internal power supply, and thus spoil the gain of the phototube during the beam pulse. This background plasma light is blocked from entering the phototube by an electro-optic gated shutter (Displaytech) that opens just before the beam pulse arrives at the scintillator. The scintillator itself is not sensitive to low-energy plasma electrons. As a result, we have been able to obtain beam pulse compression data with minimal interference from the neutralizing plasma.

A second diagnostic, a Faraday cup, is used for measurements of the current. The Faraday cup is specially designed [19] to function in a plasma environment. It consists of hole plates with hole sizes comparable to the Debye length, in order to prevent plasma from entering into the cup. The cup geometry and external circuitry are optimized to assure fast time response (<3 ns).

When the tilt voltage waveform is turned on, beam bunching is observed in the downstream diagnostic box. The degree of bunching, as well as the pulse shape, shown in Fig. 2, is clearly correlated with the voltage waveform, shown in Fig. 3. Theory specifies the ideal voltage waveform required to produce an exactly linear (versus z) velocity ramp [8, 9]. The induction module voltage waveform is optimized to obtain a rather close approximation to the ideal waveform as shown in Fig. 4.

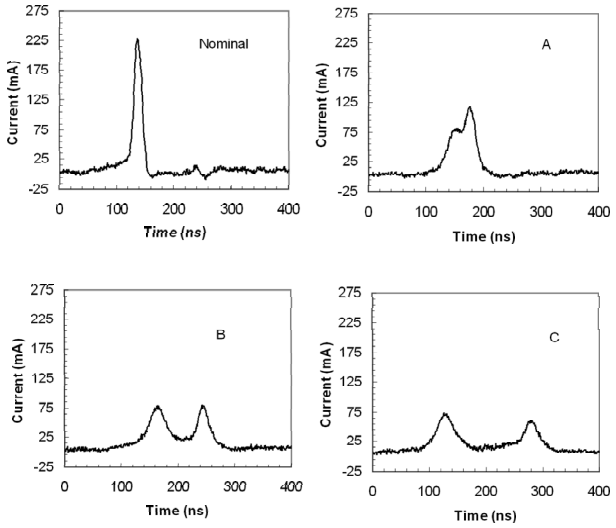

FIG. 2: Neutralized drift-compressed beam current with the voltage waveforms in Fig.3.

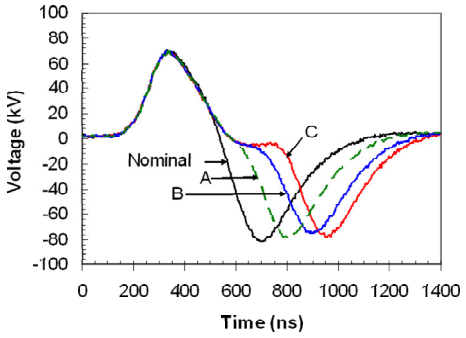

FIG. 3: Induction module voltage waveforms produced by varying the timing of the modulators.

For a given voltage waveform, the position of maximal compression is changed as the beam energy is varied. A scan in beam energy demonstrates this behavior and is shown in Fig. 5.

Thus the maximum compression is observed by fine

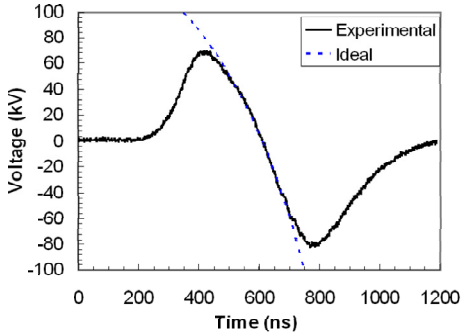

FIG. 4: Experimentally optimized and ideal induction module voltage waveforms.

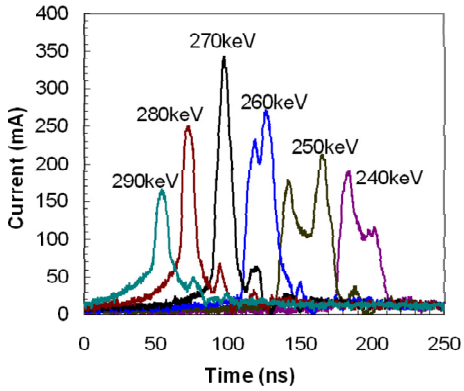

FIG. 5: Compressed beam current pulses using a nominal tilt core voltage waveform as the beam energy is varied.

tuning the beam energy to match the voltage waveform and precisely position the longitudinal focal point at the diagnostic location. This is shown in Fig. 6. The ~ 50 fold compression ratio, [see Fig. 6(b)], is obtained by taking the ratio of the signal with tilt voltage on (with compression) to the signal with tilt voltage off (without compression) [see Fig. 6(a)]. A similar result is measured with the Faraday cup [see Fig. 6(c)]. LSP calculations under these experimental conditions predict a peak compression ratio of 60 [see Fig. 6(d)].

The strong effects of neutralization are evident by comparing the compression ratio with the plasma turned on and off. Figure 7 shows that the peak current is significantly reduced when the plasma is turned off. LSP simulations under similar conditions show qualitatively similar results.

Theory predicts that the nature of beam compression is strongly dependent on the drift length [8]. As the length is increased, the compression is more sensitive to the degree of neutralization. It is also more sensitive to the intrinsic longitudinal temperature of the ion beam. Finally, if there are any instabilities, e.g. two-stream, they may become evident with longer drift lengths. Although theory predicts two-stream effects to be benign, an experimental confirmation would be desirable.

For the above reasons, we have performed additional

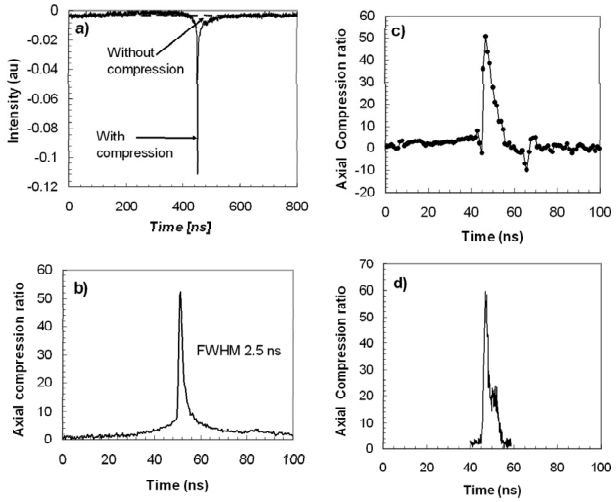

FIG. 6: (a) Measurements of beam signal using the phototube diagnostic for neutralized non-compressed, and neutralized compressed beams, (b) compression ratio obtained from the measurements using the phototube, (c) compression ratio obtained from measurements using the Faraday cup, and (d) LSP simulation for axial compression ratio under the experimental conditions.

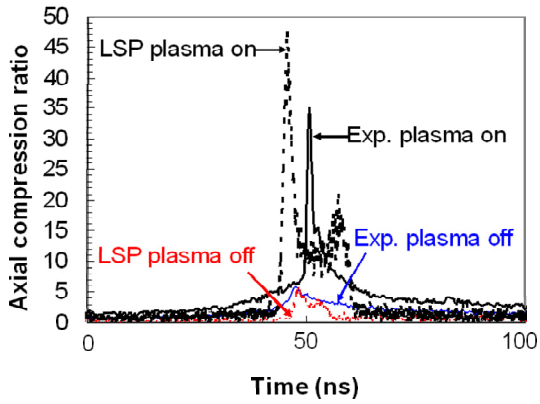

FIG. 7: Experimental data and LSP simulation of beam compression with neutralization (plasma source on) and without neutralization (plasma source off).

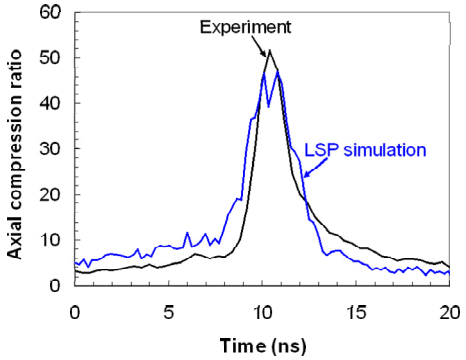

FIG. 8: Comparison of beam compression between experiment and LSP simulation for the 2-m long plasma column.

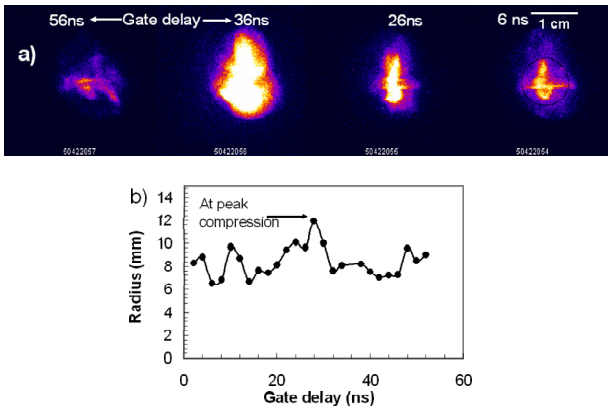

FIG. 9: Transverse images of neutralized compressed beam: (a) optical profile, and (b) beam radius. Note that the beam radius has increased at the point of maximum compression.

experiments with the drift length with plasma extended to two meters. We are able to recover the 50-fold compression in the 2-m experiment as shown in Fig. 8. The corresponding LSP simulation is also shown.

On the basis of this two-meter experiment we conclude that: 1) the degree of charge neutralization is sufficient to achieve 50 fold longitudinal compression while avoiding space-charge blow-up of the beam for the experimental configuration investigated; 2) the intrinsic longitudinal temperature is < 1eV; and 3) no collective instabilities have been observed.

Transverse as well as longitudinal compression is required to achieve the high intensity required for high energy density physics and fusion, as mentioned earlier. Simulations indicate that small spot sizes, required for fusion targets [20, 21], could be achieved with plasma neutralization [22, 23]. We have previously studied [10–13] the effects of plasma neutralization. This scaled experiment, the Neutralized Transport Experiment (NTX), demonstrated that an un-neutralized beam of several centimeter radius can be compressed transversely to $\sim$1 mm radius when charge neutralization by background plasma electrons is provided, in quantitative agreement with the simulation [14, 15].

In NDCX, optical imaging has been deployed to measure the transverse beam size as a function of time during longitudinal compression. We are able to measure the images with a 1 ns time resolution. It is interesting to observe that the transverse spot size is larger at the point of maximal compression, as shown in the Figs. 9(a) and 9(b). This feature is due to time-dependent defocusing effects occurring at the induction gap. The theory and simulations of this effect will be reported elsewhere. We are just beginning to explore combined transverse and longitudinal compression.

Acknowledgments

This Research was supported by the U.S. Department of Energy under Contract No. DE-AC02-05CH11231 with the Lawrence Berkeley National Laboratory, and Contract No. DE-AC02-76CH03073 with Princeton Plasma Physics Laboratory. We thank Dr. A. Friedman, Dr. J. Barnard, Dr. C. Celata, Dr. I. Kaganovich, Dr. E. Lee, Dr. P. Seidl and Dr. W. M. Sharp for useful discussions and comments. Thanks also to Mr. D. Baca and Mr. D. L. Vanecek for useful technical assistance.

[1] D. D.-M. Ho et al., Particle Accelerators **35**, 15 (1991).
[2] T. Kikuchi et al., Phys. of Plasmas **9**, 3476 (2002).
[3] M. J. L. de Hoon et al., Phys. of Plasmas **10**, 855 (2003).
[4] H. Qin et al., Phys. Rev. ST Accel. Beams **7**, 104201 (2004).
[5] R. C. Davidson and H. Qin, Phys. Rev. ST Accel. Beams **8**, 064201 (2005).
[6] W. M. Sharp et al., Nucl. Instrum. Meth. Phys. Res. A **544**, 398 (2005).
[7] W. M. Fawley et al., Phys. Plasmas **4**, 880 (1997).
[8] D. R. Welch et al., Nucl. Instrum. Meth. Phys. Res. A **544**, 236 (2005).
[9] C. Thoma et al., *Proc. of the 2005 Particle Accelerator Conf.*, in press (IEEE, 2005).
[10] S. S. Yu et al., in *Proc. of the 2003 Particle Accelerator Conf.*, edited by J.Chew, (IEEE, 2003), p. 98.
[11] E. Henestroza, et al., Phys. Rev. ST Accel. Beams **7**, 083501 (2004).
[12] P. K. Roy et al., Phys. of Plasmas **11**, 2890 (2004).
[13] B. G. Logan et al., Nucl. Fusion **45**, 131 (2005).
[14] C. Thoma et al., Phys. of Plasmas **12**, 043102 (2005).
[15] P. K. Roy et al., Nucl. Instrum. Meth. Phy. Res. A **544**, 225 (2005).
[16] A. Anders and G. Y. Yushkov, J. Appl. Phys. **91**, 4824 (2002).
[17] A. Anders and R. A. MacGill, Surf. Coat. Technol. **133-134**, 96 (2000).
[18] F. M . Bieniosek et al., Nucl. Instrum. Meth. Phy. Res. A **544**, 268 (2005).
[19] A. Sefkow et al., *Proc. of the 2005 Particle Accelerator Conf.*, in press (IEEE, 2005).
[20] S. S. Yu et al.,Nucl. Instrum. Meth. Phy. Res. A **544**, 294 (2005).
[21] W. M. Sharp et al., Fusion Sci. Technol. **43**, 393 (2003).
[22] D. R. Welch et al., Nucl. Instrum. Meth. Phys. Res. A **464**, 134 (2001).
[23] W. M. Sharp et al., Nucl. Fusion **44**, 221 (2004).